HHS Public Access

Author manuscript

*J Biol Inorg Chem*. Author manuscript; available in PMC 2016 May 15.

Published in final edited form as:

*J Biol Inorg Chem*. 2015 March ; 20(2): 183–194. doi:10.1007/s00775-014-1212-8.

# Electronic Structure Contributions to Reactivity in Xanthine Oxidase Family Enzymes

**Benjamin W. Stein** and **Martin L. Kirk***

Department of Chemistry and Chemical Biology, University of New Mexico, MSC03 2060, 300 Terrace St. NE, Albuquerque, NM 87131

## Abstract

We review the xanthine oxidase (XO) family of pyranopterin molybdenum enzymes with a specific emphasis on electronic structure contributions to reactivity. In addition to xanthine and aldehyde oxidoreductases, which catalyze the 2-electron oxidation of aromatic heterocycles and aldehyde substrates, this mini-review highlights recent work on the closely related carbon monoxide dehydrogenase (CODH) that catalyzes the oxidation of CO using a unique Mo-Cu heterobimetallic active site. A primary focus of this mini-review relates to how spectroscopy and computational methods have been used to develop an understanding of critical relationships between geometric structure, electronic structure, and catalytic function.

### Keywords

Molybdenum; xanthine oxidase; aldehyde oxidase; electronic structure; reactivity; carbon monoxide dehydrogenase; spectroscopy; reaction coordinate

## 1. Introduction and Scope

This mini-review focuses on the xanthine oxidase (XO) family of pyranopterin molybdenum enzymes[4–9] with a specific emphasis on recent studies that reveal how the unique electronic structure of these enzyme active sites contribute to catalysis. XO family enzymes are found in all forms of life, from simple *Archaea* to *Homo sapiens*, and they are among the most ancient enzymes found in Nature[10]. The XO enzyme family includes enzymes such as the xanthine oxidoreductases, aldehyde oxidases, nicotinate dehydrogenases, and purine hydroxylases, which catalyze the oxidative hydroxylation of a variety of heterocyclic and aldehyde substrates. Unlike the monooxygenases, which formally insert an oxygen atom derived from dioxygen into substrate C-H bonds, the molybdenum hydroxylases utilize an oxygen atom derived from metal activated water in the hydroxylation of substrates and generate rather than consume reducing equivalents in the reductive half reaction. The molybdenum dependent carbon monoxide dehydrogenase (CODH) is also a member of the XO family. Unlike other XO family enzymes that catalyze the formal insertion of an oxygen atom into a substrate C-H bond, CODH possesses a unique heterobimetallic Mo-Cu active site that functions to oxidize CO.

*Corresponding author: mkirk@unm.edu.

XOR is important from a human health standpoint, catalyzing the oxidation of hypoxanthine to xanthine and finally xanthine to uric acid. High levels of xanthine in the urine and blood are found in patients that suffer from xanthinuria (type I and type II), which is a rare genetic disorder that results from a deficiency of XOR. This can result in the formation of xanthine kidney stones and even renal failure. High serum uric acid concentrations can lead to uric acid crystallizing in the joints causing inflammation (gout). XOR and AO are involved in drug metabolism and the activation of various pro-drugs[11, 12].

## 2. General Reactions Catalyzed by XO family Enzymes

XO family enzymes catalyze the 2-electron oxidation of a wide variety of substrates according to the general equation:

$$RH+H_2O \rightarrow ROH+2H^+ +2e^-$$

where R is typically an aromatic heterocycle or an aldehyde. This reaction represents the formal insertion of an oxygen atom derived from water into a substrate C-H bond. The prototypical member of this enzyme family is xanthine oxidase, which can occur in both an oxidase (XO) and a dehydrogenase (XDH) form, with xanthine oxidoreductase (XOR) referring to the gene product. Here, we will refer to the specific enzymes as XORs and the enzyme family as the XO family. In the oxidase form (XO), XOR utilizes dioxygen as the ultimate electron acceptor to produce reactive oxygen species (ROS), while the terminal electron acceptor for the dehydrogenase form (XDH) is $NAD^+$. Oxidase activity only occurs after a reversible disulfide bond formation in the $NAD^+$ binding site[13]. XO family enzymes are widespread in biology since very few organisms are known to utilize an alternate degradation pathway for (hypo)xanthine oxidation[14, 15]. Figure 2 depicts the generally accepted catalytic cycle of XOR, and includes two of the paramagnetic species that have been detected that are of significant mechanistic importance; the *very rapid* intermediate, and the *rapid* species (type 1 and 2). The Mo active site of the AORs is structurally analogous to that found in XORs, but the two enzymes display significant differences in their substrate binding pockets that result in XORs having different substrate specificities than the AOs[12]. Other members of the XO family catalyze the oxidation of substrates such as nicotinate[16] and a variety of quinoline derivatives[17, 18] in addition to the reduction of 4-hydroxylbenzoyl-CoA[19].

A unique member of the XO family is CODH, which possesses a heterobimetallic Mo-Cu active site. Only the Mo center is redox active in the catalytic oxidation of CO to $CO_2$,

$$CO+H_2O \rightarrow CO_2+2H^+ +2e^-$$

and the Cu ion remains in the +1 oxidation state throughout the catalytic cycle. CODH also possesses hydrogenase activity, oxidizing $H_2$ to protons[20]:

$$H_2 \rightarrow 2H^+ +2e^-$$

Although the redox role of the Mo in CODH mediated catalysis is well established, the role of the Cu(I) ion in the catalytic cycle is less well understood. However, recent evidence suggests that it is likely the locus of substrate binding and initial activation, *vide infra*.

## 3. Active Site Structures

XO family enzymes have been extensively characterized structurally by X-ray crystallography and EXAFS, and these data have provided a wealth of information regarding coordination geometry, metal-ligand and Mo-Cu bond lengths, the relative orientation of the catalytically essential sulfido ligand, the nature of substrate/product binding, and key amino acid residues in the substrate binding pocket. Approximately 70 years passed between the earliest studies of XOR[21] and the first reported structure of a bacterial AO[22]. However, research efforts in the last 20 years have resulted in the publication of numerous enzyme structures in various forms, and large number of EXAFS studies on enzyme forms not amenable to crystallization. At the time of this review, there are at least 28 XOR structures that have been deposited into the protein databank (PDB)[23], the vast majority of which are from bovine XO and over half of these were published after 2010 [24]. In this section we provide a brief summary of the most recent structural studies with a specific emphasis on active site structure contributions to catalysis.

### Aldehyde Oxidase and Xanthine Oxidoreductase

The first structure of AO[22, 25] from *Desulfovibrio gigas* clearly demonstrated dithiolene coordination to Mo in addition to the various amino acid residues implicated in extensive hydrogen bonding interactions with the pyranopterin. *D. gigas* AO is a monomeric enzyme which lacks a flavin binding domain, in addition to several subtle but critical differences in the substrate binding residues. Both AO and XOR enzymes possess a catalytically essential glutamate[26] that has been suggested to serve as an active site base in the activation of a metalbound hydroxide for attack on a substrate carbon atom. However, AO and XOR differ with respect to other amino acid residues in the substrate binding pocket. Namely, AO does not possess the additional Glu and Arg residues that are present in the substrate binding region of XORs to aid in the substrate binding, activation, charge neutralization, and protonation[11].

The general structure of the XORs was known prior to the publication of the first X-ray structure from enzyme isolated from bovine milk[13] due to sequence similarities with AO, which had been structurally characterized[22]. However, the intimate details regarding the substrate binding pocket, the structure of the flavin binding domain, and the structural basis of XO/XDH interconversion were not known. XO and XDH salicylate structures demonstrated that XOR is a 290kDa homodimer, and showed the geometric relationship between the molybdenum cofactor, 2 [2Fe2S] clusters of the spinach ferredoxin variety, and FAD. The oxidase form of the enzyme differs from the dehydrogenase due to the oxidation of sulfhydryl groups in the flavin binding domain which affects both $NAD^+$ and $O_2$ binding and accessibility[13]. The wide variety of substrates oxidized by XOR have resulted in multiple studies directed toward probing the nature of the substrate binding pocket, and include structures with inhibitors (Y-700[27], FYX-051[28], allopurinol[29], TEI-6720[30])

product (urate)[31], and a variety of substrate molecules [32, 33]. Active site residues crucial to catalysis (Figure 1, left) have been determined using site-directed mutagenesis coupled with kinetic studies.[26, 34] The role(s) of these residues in productive substrate orientation has been considered in detail and is a matter ongoing debate. Mechanistic arguments[34] involving Arg 880 stabilizing a built-up of charge on the substrate following nucleophilic attach by the metal-bound hydroxide favor an "upside" orientation (Figure 4). Conversely, urate-bound structures[31] display an "upside-down" orientation. These issues regarding substrate orientation have recently been addressed using detailed QM/MM calculations[2] (see Section 5).

### Carbon Monoxide Dehydrogenase (CODH)

The crystal structure shows it to be a 277 kDa homodimer consisting of three subunits; the molybdoprotein domain, a [2Fe-2S] cluster domain, and a FAD containing domain. The overall sequence homology with XOR is very high, with the molybdoprotein domain being 57% similar[35]. The electron transport chain of CODH is nearly identical to that observed in XOR, suggesting electrons are shuttled from the active site through the pyranopterin dithiolene, the two [2Fe-2S] clusters, flavin, and finally to the exogenous redox cofactor, a b-type cytochrome. The catalytic domain possesses a biologically unique heterobimetallic Mo-Cu active site containing a Mo ion that redox cycles between the Mo(IV) and Mo(VI) oxidation states. The Mo ion is bridged by a μ-sulfido ligand to a Cu(I) center [36], prompting questions regarding the interplay between these two metals in catalysis. Interestingly, the oxidized form the enzyme contains $d^0$ Mo(VI) and $d^{10}$ Cu(I) ions and the large oxidation state differential between the two metal ions represents a difference of 10 d-electrons. The electronic structure consequences of this remarkable $[Mo\text{-}S\text{-}Cu]^{5+}$ center have been discussed in the context of covalent 3-center bonding interactions[1, 37]. In addition to the native protein, an inhibited structure was reported with *n*-butylisocyanide bound to the bimetallic center. This structure revealed the presence of a Mo-S-C-O heterocycle, which has led to interesting inhibitor-based mechanistic hypotheses, involving analogous C-S bonded intermediates, for the catalytic conversion of CO to $CO_2$. The *n*-butylisocyanide structure has provided important mechanistic insight since it clearly indicates a potential role for the Cu(I) site in substrate binding and the resulting formation of an organometallic Cu carbonyl intermediate. Spectroscopic studies on XO clearly indicate the presence of C-S bond formation in the aldehyde inhibited species. Coupled with the inhibitory nature of the *n*-butylisocyanide CODH complex, C-S bond formation in the catalytic cycle of any XO family enzyme must be carefully scrutinized due to the inherent stability of this bond.

## 4. Spectroscopic Studies

Enzyme structural studies represent the starting point for understanding the catalytic mechanism of all XO family enzymes. When information gleaned from X-ray crystallography and EXAFS are coupled to spectroscopic studies, detailed insight into enzyme active site electronic structure contributions to catalysis begin to emerge. Unfortunately, XO family enzymes have been very difficult to study using spectroscopic methods common for other metalloenzymes[38, 39]. This derives from the fact that the

stable Mo(IV) and Mo(VI) oxidation states are *diamagnetic*, precluding their study using paramagnetic spectroscopies such as electron paramagnetic resonance (EPR), electron nuclear double resonance (ENDOR) and other pulsed EPR techniques, and magnetic circular dichroism (MCD) spectroscopy. Electronic absorption spectroscopy is a primary technique used to provide the most basic metalloenzyme electronic structure information, but its use in the study of XO family enzymes has been limited due to the presence of strongly absorbing 2Fe2S clusters and FAD. These same intense absorption bands, coupled with the fluorescence of free FAD, also severely limit the utility of resonance Raman spectroscopy for the study the Mo site. Thus, the bulk of spectroscopic studies on pyranopterin Mo enzymes that have provided detailed electronic structure information and mechanistic insight have been EPR based techniques that have probed $d^1$ Mo(V) inhibited states and trapped catalytic intermediates. Here we highlight specific spectroscopic studies that have greatly contributed to our understanding of Mo hydroxylase and CODH electronic structure and reactivity.

## Xanthine Oxidoreductase

XOR has been thoroughly studied by paramagnetic resonance probes (EPR/ENDOR) of the Mo(V) state. Although far fewer optical studies (MCD, electronic absorption, resonance Raman) have been performed on XORs, the information content of these studies has been high. XORs can form multiple paramagnetic species during the reaction with purines or aldehydes (Figure 2) and these have been examined in order to gain insight into active site geometric and electronic structure, and enzyme mechanism. The vast majority of these spectroscopic studies have been performed on bovine XO due to the large number of EPR active enzyme forms and the high stability of the protein under a variety of conditions. Four well-characterized EPR detectable species have been observed as a function of incubation time with added substrate. These are variously termed *aldehyde inhibited*, *slow* (desulfo form), *rapid*, and *very rapid* (Figure 5). The *very rapid* intermediate is a Mo(V)-product complex that results from a bifurcation in the catalytic pathway. The *rapid* type I and II species are believed to be paramagnetic analogues of the Michaelis complex that represent different orientations of the substrate in the binding pocket but not directly coordinated to the Mo center[40]. The *desulfo* form of XO can be generated by cyanide treatment, which removes the catalytically essential terminal sulfido ligand. Under specific conditions, dithionite reduction of this catalytically inactive enzyme form yields the *slow* EPR signal[41]. Here, we will focus our attention on the catalytically relevant *very rapid* species, recent studies on *aldehyde inhibited* XO, and resonance Raman studies of product-bound XOR[42].

The *very rapid* catalytic intermediate is formed with specific substrates (i.e. xanthine, 2-hydroxy-6-methylpurine), directly precedes the formation of the oxidized Mo(VI) state in the oxidative half reaction, and has conclusively been shown to arise from a Mo(V)-product bound species. EPR spectra of the $^{33}S$ enriched *very rapid* intermediate display strong hyperfine coupling to a single $^{33}S$ nucleus, and this has been used to estimate the degree of Mo=S covalency in the singly occupied molecular orbital (SOMO or redox orbital). The estimated ~38% sulfido character[43] in the formally Mo(xy) redox orbital indicates that the oxidized active site also possesses a highly delocalized $Mo^{VI}$-$S_{Sulfido}$ π* bonding

interaction. This is important since the $Mo^{VI}$-$S_{Sulfido}$ π* redox active molecular orbital is the acceptor orbital in the two electron oxidation of XOR substrates and suggests an electronic structure role for the catalytically essential sulfido ligand. Initial $^{17}O$ and $^{13}C$ ENDOR experiments[44] were used to suggest the presence of a Mo-$C_{Product}$ bond in *very rapid*. However, a subsequent $^{13}C$ ENDOR study[45] showed that *very rapid* does not possesses a Mo-$C_{Product}$ bond, rather the product is bound to the Mo ion as the enolate tautomer. The observation of a Mo-O-$C_{Product}$ linkage is important since it has been shown by $^{17}O$ labeling that the bridging oxygen originates from a coordinated hydroxyl ligand ($Mo^{VI}$-OH), providing support for a hypothesis that substrate oxidation is initiated by nucleophilic attack of metal activated water on the substrate C atom that is hydroxylated.

MCD spectroscopy of the *very rapid* species[46] was used to show that the Mo≡O group in XO is oriented in an apical position relative the dithiolene S donors, a coordinated hydroxide, and the terminal equatorial sulfido (Mo=S). The observation of an equatorial sulfido ligand by MCD was contrary to X-ray crystallographic studies that suggested the terminal sulfido was oriented in the apical position and the oxido donor was located in the equatorial plane. Higher resolution X-ray crystal structures are now in full agreement with this bonding description [28]. Thus, the picture that emerged from these studies indicates that a *cis*-[$Mo^{VI}$OS] active site with an equatorial sulfido ligand is poised to formally accept a hydride from substrate to form a reduced [$Mo^{IV}$O(SH)]-product complex. Product release, binding of a water molecule, and subsequent $2e^-/2H^+$ transfer then yields the catalytically competent [$Mo^{VI}$OS] active site.

The geometric and electronic structure of *aldehyde inhibited* XO has been recently probed at high resolution by ENDOR[47] and EPR[48] spectroscopies. Although it was known that *aldehyde inhibited* XO displayed hyperfine coupling to $^{17}O$, $^{33}S$, $^{13}C$, and $^{1,2}H$ nuclei, the general structure of this species had not been unambiguously determined until recently[47]. An unusual aspect of the paramagnetic resonance spectra is the observation of strong and isotropic $^{13}C$ hyperfine coupling to the carbonyl carbon of the aldehyde. Although originally interpreted as arising from a Mo(V)-C bond[44], a more recent $^{1,2}H$ ENDOR study[47] clearly showed that the structure resulted from a Mo(-O-C-S-) four membered chelate ring with a tetrahedral C center. The idea of Mo-C bond formation in the catalytic cycles of XO family enzymes is not new, having been previously postulated for the XO "very rapid" intermediate based on ENDOR data[44]. However, later ENDOR studies clearly revealed that this is not the case, with the "very rapid" intermediate possessing a Mo-O-$C_{product}$ linkage[45]. A subsequent EPR and computational study[48] on *aldehyde inhibited* XO was then used to determine the relative orientation of the $^{95,97}Mo$ ($\mathbf{A^{Mo}}$), $^{13}C$ ($\mathbf{A^{C}}$), and g tensor components to the Mo-ligand bonds. This analysis concluded that the Mo→C spin delocalization that leads to the large $^{13}C$ hyperfine interaction derives from an asymmetric bonding interaction in the Mo(-O-C-S-) chelate. Interestingly, this study related the tetrahedral carbon center in *aldehyde inhibited* XO with the proposed tetrahedral transition state/intermediate in the oxidation of XO enzyme substrates to show the plausibility of an important Mo-$O_{eq}$-C delocalization pathway that could contribute to electron transfer between the Mo site and the substrate to lower the energy of the transition state along the reaction coordinate. As such, *aldehyde inhibited* XO is a rudimentary paramagnetic

analogue of the tetrahedral intermediate/transition state along the reaction coordinate, and this highlights the importance of Mo-$O_{eq}$-C delocalization to enzymatic catalysis.

Reacting oxidized XO/XDH with lumazine and lumazine derivatives has been shown to result in a strongly absorping Mo(IV)→product metal-to-ligand charge transfer (MLCT) complex with long-wavelength absorption and a large resonance enhancement of in-plane product stretching modes[42]. Coupled with the earlier MCD work[46], this shows the importance of having the substrate/product being oriented in the same plane as the Mo≡O vector in order to couple the equatorial "in-plane" Mo(xy) redox orbital with the π-system of the product in the reductive half reaction. The near IR rR data on Mo-product complexes with 4-thioviolapterin and 2,4-dithioviolapterin reveal the presence of resonantly enhanced, low-frequency Mo-(pyranopterin ditholene) modes. Since the Mo(IV)→product MLCT generates a transient hole on the Mo center (formally Mo(V) in the MLCT state), the explicit observation of resonantly enhanced pyranopterin dithiolene vibrational modes strongly suggests that the pyranopterin dithiolene is very responsive to Mo redox changes and provides an efficient electron transfer conduit in the oxidative half reaction of the enzyme.

## Carbon Monoxide Dehydrgenase (CODH)

Compared to the extensive studies on XOR, spectroscopic studies on CODH are limited. This is a direct result of the smaller number of Mo(V) species that have been generated for CODH [3, 20, 49], in addition to the inherent problems associated with additional chromophores common to all XO family enzymes. Chemical reduction of CODH by dithionite, CO, or $H_2$ yields a Mo(V) EPR signal that displays a nearly isotropic coupling to the diamagnetic $^{63,65}$Cu nucleus. A combination of $^{13}$C and $^{63,65}$Cu ENDOR on the CO species, coupled with spectroscopic and bonding calculations [3] on a variety of trial structures (Figure 6) have been used to determine putative structures for the signal giving species. Calculated spin-Hamiltonian parameters were then used to eliminate unlikely structures for the spectroscopic intermediate. It was suggested that $MoO_2$ dioxo species are unlikely candidates for this intermediate due to the resulting ligand field causing a severe reduction in the g-values, which are inconsistent with the experimental results. The spin-Hamiltonian computations demonstrated that the structure most consistent with the EPR signal-giving species is a modification of a CO bound species (Figure 6, structure 1), and the S-Cu-$S_{Cys}$ angle was found to be of critical importance. As S-Cu-$S_{Cys}$ angle deviates from 180°, the Cu sp hybridization increases, resulting in an increase in the Cu hyperfine anisotropy. Due to this effect structures **2** and **3** are anticipated to display very rhombic hyperfine anisotropy. However, the calculated g- and $^{13}$C hyperfine tensors are in very good agreement with experiment, providing strong supports for structure **1** as the signal giving species. This is important, as structure **1** represents a paramagnetic analogue of the starting point in the catalytic cycle following binding of substrate. An additional structure was studied computationally, representing a product bound (bicarbonate) species (**4**). Interestingly, this product bound Mo(V) species is analogous to the *very rapid* EPR signal seen in XOR enzymes.

## 5. The Enzyme Reaction Coordinate

XO family enzymes have been the subject of multiple computational studies, and these include early *ab initio* calculations using formaldehyde as a substrate, progressing to more advanced calculations that explicitly include the effects of the protein environment using QM/MM methodologies. Two primary mechanisms have been proposed as the most likely candidates for the reaction of XO family enzymes with aldehyde and purine substrates. The first is a concerted mechanism that involves simultaneous nucleophilic attack of the Mo-bound hydroxide and a formal hydride transfer from the substrate to the catalytically essential sulfido ligand on Mo, while the second is proposed to be a step-wise mechanism that involves the formation of a stable tetrahedral intermediate prior to the formal hydride transfer. Significant variations of these two mechanisms have been proposed[50, 51] but these suffer from an incomplete description of the reaction coordinate or very large energy barriers.

### Xanthine Oxidoreductase

Based on biochemical studies of the reaction of XO with xanthine[52], the kinetic mechanism of XO may be written as

$$XO(Mo^{\mathrm{VI}})+\mathrm{Xanthine} \rightleftharpoons XO(Mo^{\mathrm{VI}})\cdot\mathrm{Xanthine} \xrightarrow{k_r} XO(Mo^{\mathrm{VI}})\cdot\mathrm{Urate} \xrightarrow{k_d} XO(Mo^{\mathrm{IV}})+\mathrm{Urate}$$

where $k_r$ is the rate of enzymatic reduction and $k_d$ is the rate of product release. These rates have been determined for both the XDH[26, 34, 53] and XO[52, 54–58] forms of XOR, with product release being rate limiting at lower temperatures but enzyme reduction becoming rate limiting near physiological temperature[52]. Reported barrier heights of enzyme reduction vary slightly, but are ~16 kcal/mol for XO and ~14 kcal/mol for XDH. Theoretical studies have helped to clarify the reaction mechanisms of XOR and AO by discriminating between the step-wise (nucleophilic attack on substrate followed by hydride transfer) and concerted (simultaneous attack and transfer) mechanisms. The step-wise mechanism has been found to be highly favored for both AO and XO (*vide infra*), reflecting the strongly homologous nature of these two enzymes.

With few exceptions, theoretical studies on XO have focused on the reaction with aldehydes. This is due to the simplicity of the aldehyde structure, in addition to complications involved with varied substrate orientations, multiple substrate hydrogen bonding interactions with active site residues, and the numerous tautomeric forms of N-heterocyclic substrates. The studies using aldehyde substrates have yielded a consensus mechanism that involves the formation of a tetrahedral intermediate followed by rate limiting formal hydride transfer, which results in the reduction of the Mo center. The mechanism of xanthine oxidation has been found to be quite similar, but the tetrahedral intermediate was found to be at high energy and only marginally stable.

### Density Functional Theory (DFT) Studies

Density functional theory studies of XOR family enzyme reactivity have primarily focused on the oxidation of formaldehyde (HCHO), acetaldehyde ($CH_3CHO$), formamide

($HCONH_2$), or formamidine ($HC(=NH)NH_2$). The first DFT study on the reaction of XO with aldehydes[50] suggested hydroxyl transfer to a Mo-C bonded formaldehyde, a structure consistent with some EPR work on the XO *very rapid* intermediate [44]. This mechanism was contrasted in a computational study[59] that proposed nucleophilic attack of the equatorial hydroxido to form a tetrahedral intermediate (Figure 2), followed by rate limiting hydride transfer to generate the Mo(IV)-sulfhydryl species. Later work[61] compared concerted and stepwise versions of the reaction mechanism proposed in [59], with HCHO, $CH_3CHO$, and $HC(=NH)NH_2$ as substrates, with HCHO being the most reactive. These calculations favored a concerted mechanism, where nucleophilic attack on the substrate carbonyl carbon occurs simultaneously with hydride transfer to the terminal sulfido. This interpretation is consistent with KIE studies that show at least some degree of C-H bond scission at the transition state. A combined *ab initio* and DFT study[51] used advanced computational methodologies to study the reaction with $HCONH_2$ as substrate and found very large reaction barriers, making it difficult to favor a particular mechanism.

## QM/MM Studies on AO

The disagreement between the QM studies probing the reaction coordinate of XO with aldehydes led to a series of QM/MM studies[62, 63] on the reaction of AOR with acetaldehyde. These studies were of interest since they incorporated the conserved catalytically essential active site glutamate (Glu869) in the reaction. Three QM regions were compared: 1) Mo cofactor (Moco) and substrate, 2) Moco, substrate, and Glu869, and 3) Moco, substrate, Glu869, and a water molecule hydrogen bound to Glu869 and substrate. A number of mechanistic pathways were considered, differing in whether the reaction was concerted or stepwise, The results of this study were quite informative, with the stepwise base-promoted pathway (pathway C in [62]) having the lowest activation barrier of 8.5 kcal/mol. During this reaction Glu869 serves as a Lewis base to facilitate nucleophilic attack on the substrate carbonyl carbon to form a tetrahedral intermediate. This intermediate then transfers a hydride to the Mo bound sulfido ligand resulting in enzyme reduction. More advanced free energy perturbation (FEP)/MM calculations[63], which enable the determination of the free-energy reaction profile, support this mechanistic conclusion.

## QM/MM studies of XOR

Two QM/MM studies[2, 65] were performed on XOR that examined the role of active site residues in facilitating substrate binding and transition state stabilization, cofactor changes and their effect on catalysis, and the reactivity of alternate substrates. Contrary to AO, where only the conserved glutamate was found to play a pivotal role, XOR utilizes several substrate binding residues to stabilize the complex charge buildup on xanthine during the course of catalysis. Several studies[31–33] have been performed which attempt to determine the particular orientation of substrate during catalysis, the so-called “upside” and “upside down” orientations (Figure 4), primarily through the examination of crystal structures and the kinetic behavior of specific variants. QM/MM calculations show that the thermodynamically favored reactant species is the “upside” configuration, in agreement with the published crystal structures. However, modeling the reaction path with both orientations shows that the “upside-down” orientation is kinetically favored for catalysis. This was rationalized by the stabilization of the excess charge on xanthine by Arg880 (Figure 7).

## The Catalytically Essential Sulfido

The $C_{substrate}$-H bond-breaking step along the reaction coordinate may be thought of as the *formal* transfer of a hydride from the substrate to the Mo=S sulfido ligand, and this results in the formation of a Mo(IV)-SH sulfhydryl species. Alternatively, this process can be described as a two-electron reduction of the Mo(VI) ion that is coupled to the protonation of the terminal sulfido.[66] Thus, XO mediated substrate oxidations are of keen mechanistic interest due to the fact that the $C_{substrate}$-H proton and two electrons can be transferred to the $Mo^{VI}$=S unit as a single entity (hydride), as a sequential or coupled two electron-proton transfer, or by a radical-type process involving the transfer of an H-atom and an electron. The complex nature of the $C_{substrate}$-H bond-breaking step is governed by the nature of the catalytically essential sulfido, which forms an integral component of the Mo=S π* redox orbital in the Mo(VI) and Mo(V) oxidation states. The Mo=$S_{sulfido}$ bond is *highly* covalent, as evidenced by the large $g_1$ observed in the EPR spectra of XO *very rapid*. The large $g_1$ indicates significant charge transfer and covalency contribution to the Mo=$S_{sulfido}$ bonding scheme, and this is important for facilitating the formal hydride transfer process that results in C-H bond cleavage, substrate oxidation, Mo reduction, and the formation of a Mo(IV)-SH species in reduced enzyme.

Electron occupation of the Mo=S π* redox orbital affects the relative electro-/nucleophilic nature of the terminal sulfido and provides support for a mechanism that is under orbital control. An analysis of the wavefunction along the XO reaction coordinate reveals that the substrate $C_{substrate}$-H hydrogen that is transferred to the terminal sulfido *does not* possess hydridic character. This is evidenced by the fact that there is not a doubly occupied frontier molecular orbital that has appreciable H 1s orbital character along the $C_{substrate}$-H bond-breaking segment of the reaction coordinate, and this hydrogen is transferred with near zero charge. Initial evidence for a coupled $2e^-/H^+$ transfer mechanism resulted from an analysis of the XO wavefunction at the transition state as a function of substrate. Occupation of the Mo=S π* redox orbital along the reaction coordinate will increase the nucleophilicity of the terminal sulfido and allow for the $C_{substrate}$-H hydrogen to be transferred as a proton.

## Computational Studies on CODH

Kinetic studies of CODH[49] give an activation energy of 11.4 kcal/mol at pH 7.2, corresponding to a $k_{cat}$ of 93.3 $s^{-1}$. Furthermore, CO oxidation is not limited by CO concentration, which demonstrates rapid and efficient binding of CO to the active site. This site of CO binding is generally accepted to be the Cu(I) site, which yields an organometallic Michaelis complex. Only a few computational studies have been performed on the mechanism of CODH. The first computational study of CODH[67] proposed two mechanisms on the basis of DFT results, one of which was based upon the crystallographic observation of a C-S bond in the *n*-butylisocyanide inhibited structure. Although this structure is particularly stable, it does demonstrate the possibility of C-S bond formation during catalysis. The second mechanism involves nucleophilic attack on the substrate carbon by an equatorial oxido ligand, followed by extrusion of a molecule of $CO_2$. Due to the absence of C-S bond formation in this mechanism, the authors proceeded to propose that the substrate carbon migrates to the sulfido, followed by copper migration to the substrate oxygen. A molecule of water was found to be necessary for product release. This mechanism

resulted the formation of a very stable S-C bonded thiocarbonate intermediate. This was rationalized by considering the activation energy relative to two full catalytic cycles. Here, the energetics were found to be slightly more favorable, with an overall reaction barrier of 18.9 kcal/mol.

A second DFT study[68] was subsequently published that detailed a qualitatively similar mechanism and compared the oxidation of CO and MeNC. Importantly, due to unfavorable energetics these authors suggested a thiocarbamate intermediate was unlikely to be relevant to the enzyme mechanism. The thiocarbamate intermediate was shown to exergonically form when isonitriles are used as substrates, and is strongly inhibitory with a barrier of at least 24 kcal/mol (CO) or 33 kcal/mol (MeNC). These calculated kinetic barriers represent a lower bound, as no transition state was located for the breakdown of these intermediates.

A more recent DFT study[1] focused on specific orbital interactions that are unique to the CODH active site and how these are involved in the activation of CO for oxidation. An interesting similarity was found between the mechanism of CODH and previous work on XO[48]. Here, it was suggested that CODH utilizes Cu(I) not only for substrate binding, but as a “pseudo-hydrogen” where the C-Cu bond is cleaved in a manner almost identical to that observed for the cleavage of C-H bonds in XO. A Cu-bound hydroxide was found to facilitate the release of product as bicarbonate, with an activation barrier of 12 kcal/mol. Importantly, the formation of an inhibitory C-S bond is avoided in this mechanism (Figure 8).

A picture of how CO may be oxidized by CODH that avoids the formation of inhibitory C-S bonds is beginning to emerge, and this description is based upon our knowledge of electronic structure contributions to catalysis in XOR. Although it was initially suggested[67] that the formation of a stable C-S bond is an essential element of the catalytic cycle, there has been disagreement on this point[68] based on the fact that such C-S bonded structures tend to represent inhibited enzyme forms in XO family enzymes. Structural similarities between the *n*-butylisocyanide CODH structure and XO *aldehyde inhibited* (Figure 5) support the stability and non-reactivity of cyclic intermediates that possess C-S bonds in XO family enzymes. A recent computationally based mechanism has been proposed that has provided a convenient Lewis structure description of the catalytic cycle (Figure 8). Here, the chemical reactivity has been described in the context of C-Cu(I) σ-bond cleavage (Figure 9), which is analogous to the C-H bond breaking step observed in XO[48].

## 6. Donor-Acceptor Contributions to Bond Activation and Transition State Stabilization in XOR and CODH

Transition state calculations have provided important information regarding key intermediates and transition states along the reaction coordinate. However a molecular level bonding description of how the active site contributes to the activation and scission of the substrate C-H bond is important to understanding the relationship between enzyme active site geometric and electronic structure contributions to catalysis. A natural bond orbital (NBO) analysis has been used to develop new insight into electronic structure contributions to C-H bond activation and transition state stabilization in XO have shown that important

charge transfer interactions function to reduce repulsive interactions along the reaction coordinate. NBOs are localized bonding orbitals that possess maximum electron density, and they provide a means of linking quantum chemical calculations with chemically intuitive Lewis structures and valence bond descriptions of the reaction coordinate in addition to delineating the primarly delocalizations responsible for deviations from this Lewis description. We have discussed the importance of the catalytically essential sulfido ligand in the Mo hydroxylases in terms of a very covalent Mo=S bonding scheme in the enzymes. This Mo=S bonding scheme contributes to the unique electronic structure of the active site that uses a combination of C-H $\sigma \rightarrow$ Mo=S $\pi$ * and Mo=S $\pi \rightarrow$ C-H $\sigma$* donations to activate substrate C-H bonds. These charge transfers effectively reduce the C-H bond order by decreasing the electron density in the C-H bonding orbital and populating the C-H $\sigma$* antibonding orbital through back donation from the Mo=S $\pi$ bonding orbital. The net effect is an activation of the C-H bond for cleavage along the reaction coordinate. At the transition state a $O_{eq} \rightarrow$(Mo + C) charge transfer interaction that derives from Mo-$O_{eq}$-$C_{substrate}$ bonding is the most important contribution to transition state stabilization. The importance of the Mo-$O_{eq}$-$C_{substrate}$ bonding interaction to catalysis is supported by EPR studies on XO aldehyde inhibited that show Mo-$O_{eq}$-C delocalization contributes to the large $^{13}$C hyperfine interaction at the tetrahedral carbon center. The importance of the a $O_{eq} \rightarrow$(Mo + C) charge transfer interaction to transition state stabilization derives from how this charge transfer interaction reduces electronic repulsions as the transition state is approached, effectively reducing the classical energy barrier to product formation.

A similar natural bond orbital (NBO) analysis of the CODH reaction coordinate indicates that the cyclic intermediate in Figure 8 (structure **3**), is a 50:50 resonance hybrid of formal Mo(VI) and Mo(IV) structures that derives from a combination of C-Cu $\sigma \rightarrow$ Mo-S $\pi$* and Mo-S $\pi \rightarrow$ C-Cu $\sigma$* donations. What is particularly interesting is the remarkable similarity to the forward and back charge donations in XO that function to activate the C-H bond for catalysis. This is exemplified by comparing the resonance structures that contribute to the ground states of the CODH and XO intermediates and comparing the CODH NBOs that are involved in Cu-C $\sigma \rightarrow$ Mo-S $\pi$* and Mo-S $\pi \rightarrow$ Cu-C $\sigma$ * delocalization with the corresponding MOs in XO (Figure 9). In summary, the molecular orbital analyses for CODH and XO have provided detailed new insight into their mechanisms, and show that electronic structure contributions to reactivity in CODH essentially mirror those that are operative in the molybdenum hydroxylases, providing a link between C-H bond activation and CO activation in these remarkable XO family enzymes.

## 7. Conclusions and outlook

The relationship between unique spectroscopic features and the geometric and electronic structure of XO family enzyme active sites has revealed key components of the bonding scheme that are essential to catalysis. Catalytic cycles for XORs and CODH that are based on sound electronic structure descriptions are now beginning to emerge. Although XO, AO, CODH are different XO family enzymes, they all possess a catalytically essential sulfido (either terminal or bridging) that contributes to Mo redox, C-H bond scission and S-H bond formation, lowering the transition state energy, and a reduction of charge buildup along the reaction coordinate. Unique donor-acceptor interactions have been revealed that lead to

powerful valence bond descriptions XO and CODH reactivity that share a remarkable similarity.

Remarkable progress has been made over the past decade regarding our understanding of the complex relationships that exist between the underpinning active site electronic structure and reactivity patterns observed in XO family enzymes. Recent work[42, 69] points toward open questions regarding the specific role of pyranopterin in the catalytic cycles of these enzymes and future studies will continue to probe the nature of the unique and electronically complex ligand. Intriguing questions remain regarding how substrate orientation in the binding pocket affects the reaction kinetics of the reductive, and potentially even the oxidative, half reactions of XORs. Additional studies will be required to fully assess the role of the bridging sulfide and the Cu(I) ion in CODH, including experiments specifically designed to test mechanistic hypotheses that have been proposed for this remarkable enzyme. Finally, there are numerous other XO family enzymes that catalyze reactions with a diverse range of substrates (see section 2 for examples), and it will be interesting to determine how the key electronic structure contributions to catalysis outlined here may be used to fully explain their mechanisms of reactivity.

## Abbreviations

| | |
|---|---|
| **AO** | Aldehyde oxidase |
| **CODH** | CO dehydrogenase |
| **DFT** | Density functional theory |
| **ENDOR** | Electron-nuclear double resonance |
| **EPR** | Electron paramagnetic resonance |
| **EXAFS** | Extended X-ray absorption fine structure |
| **FAD** | Flavin adenine dinucleotide |
| **MCD** | Magnetic circular dichroism |
| **ROS** | Reactive oxygen species |
| **QM/MM** | Quantum mechanics/molecular mechanics |
| **rR** | Resonance Raman |
| **XDH/XO/XOR** | Xanthine dehydrogenase/oxidase/oxidoreductase |

## References

1. Stein BW, Kirk ML. Chem. Commun. 2014; 50:1104–1106.
2. Metz S, Thiel W. J. Am. Chem. Soc. 2009; 131:14885–14902. [PubMed: 19788181]
3. Shanmugam M, Wilcoxen J, Habel-Rodriguez D, Cutsail I, George E, Kirk ML, Hoffman BM, Hille R. J. Am. Chem. Soc. 2013 131119100231003.
4. Hille R, Hall J, Basu P. Chem. Rev. 2014
5. Hille R. Dalton Trans. 2013; 42:3029–3042. [PubMed: 23318732]
6. Hille R, Nishino T, Bittner F. Coord. Chem. Rev. 2011; 255:1179–1205. [PubMed: 21516203]
7. Hille R. Arch. Biochem. Biophys. 2005; 433:107–116. [PubMed: 15581570]

8. Hille R. Chem. Rev. 1996; 96:2757–2816. [PubMed: 11848841]
9. Kirk, ML.; Stein, B. Comprehensive Inorganic Chemistry II. Second. Reedijk, J.; Poeppelmeier, K., editors. Amsterdam: Elsevier; 2013. p. 263-293.
10. Workun GJ, Moquin K, Rothery RA, Weiner JH. Microbiol. Mol. Biol. Rev. 2008; 72:228–248. [PubMed: 18535145]
11. Pryde DC, Dalvie D, Hu Q, Jones P, Obach RS, Tran T-D. J. Med. Chem. 2010; 53:8441–8460. [PubMed: 20853847]
12. Kitamura S, Sugihara K, Ohta S. Drug Metabolism and Pharmacokinetics. 2006; 21:83–98. [PubMed: 16702728]
13. Enroth C, Eger BT, Okamoto K, Nishino T, Nishino T, Pai EF. Proc. Natl. Acad. Sci. U.S.A. 2000; 97:10723–10728. [PubMed: 11005854]
14. Li M, Muller TA, Fraser BA, Hausinger RP. Arch. Biochem. Biophys. 2008; 470:44–53. [PubMed: 18036331]
15. Montero-Moran GM, Li M, Rendon-Huerta E, Jourdan F, Lowe DJ, Stumpff-Kane AW, Feig M, Scazzocchio C, Hausinger RP. Biochemistry. 2007; 46:5293–5304. [PubMed: 17429948]
16. Wagener N, Pierik AJ, Ibdah A, Hille R, Dobbek H. Proc. Natl. Acad. Sci. U.S.A. 2009; 106:11055–11060. [PubMed: 19549881]
17. Canne C, Stephan I, Finsterbusch J, Lingens F, Kappl R, Fetzner S, Hüttermann J. Biochemistry. 1997; 36:9780–9790. [PubMed: 9245410]
18. Tshisuaka B, Kappl R, Huettermann J, Lingens F. Biochemistry. 1993; 32:12928–12934. [PubMed: 8251516]
19. Gibson J, Dispensa M, Harwood CS. J. Bacteriol. 1997; 179:634–642. [PubMed: 9006014]
20. Wilcoxen J, Hille R. J. Biol. Chem. 2013
21. Dixon M, Thurlow S. Biochem. J. 1924; 18:976–988. [PubMed: 16743383]
22. Romão MJ, Archer M, Moura I, Moura JJG, LeGall J, Engh R, Schneider M, Hof P, Huber R. Science. 1995; 270:1170–1176. [PubMed: 7502041]
23. http://www.pdb.org.
24. Dobbek H. Coord. Chem. Rev. 2010; 255:1104–1116.
25. Rebelo JM, Dias JM, Huber R, Moura JJ, Romao MJ. J. Biol. Inorg. Chem. 2001; 6:791–800. [PubMed: 11713686]
26. Leimkühler S, Stockert AL, Igarashi K, Nishino T, Hille R. J. Biol. Chem. 2004; 279:40437–40444. [PubMed: 15265866]
27. Fukunari A, Okamoto K, Nishino T, Eger BT, Pai EF, Kamezawa M, Yamada I, Kato N. J. Pharmacol. Exp. Ther. 2004; 311:519–528. [PubMed: 15190124]
28. Okamoto K, Matsumoto K, Hille R, Eger BT, Pai EF, Nishino T. Proc Natl Acad Sci U S A. 2004; 101:7931–7936. [PubMed: 15148401]
29. Okamoto K, Eger BT, Nishino T, Pai EF, Nishino T. Nucleosides Nucleotides Nucleic Acids. 2008; 27:888–893. [PubMed: 18600558]
30. Okamoto K, Eger BT, Nishino T, Kondo S, Pai EF, Nishino T. J. Biol. Chem. 2003; 278:1848–1855. [PubMed: 12421831]
31. Okamoto K, Kawaguchi Y, Eger BT, Pai EF, Nishino T. J. Am. Chem. Soc. 2010; 132:17080–17083. [PubMed: 21077683]
32. Pauff JM, Zhang J, Bell CE, Hille R. J. Biol. Chem. 2008; 283:4818–4824. [PubMed: 18063585]
33. Cao H, Pauff JM, Hille R. J. Biol. Chem. 2010; 285:28044–28053. [PubMed: 20615869]
34. Pauff JM, Hemann CF, Jünemann N, Leimkühler S, Hille R. J. Biol. Chem. 2007; 282:12785–12790. [PubMed: 17327224]
35. Dobbek H, Gremer L, Meyer O, Huber R. Proc Natl Acad Sci U S A. 1999; 96:8884–8889. [PubMed: 10430865]
36. Dobbek H, Gremer L, Kiefersauer R, Huber R, Meyer O. Proc Natl Acad Sci U S A. 2002; 99:15971–15976. [PubMed: 12475995]
37. Gourlay C, Nielsen DJ, White JM, Knottenbelt SZ, Kirk ML, Young CG. J. Am. Chem. Soc. 2006; 128:2164–2165. [PubMed: 16478141]

38. Solomon EI, Szilagyi RK, DeBeer George S, Basumallick L. Chem. Rev. 2004; 104:419–458. [PubMed: 14871131]
39. Solomon EI. Inorg. Chem. 2006; 45:8012–8025. [PubMed: 16999398]
40. Gutteridge S, Tanner SJ, Bray RC. Biochem. J. 1978; 175:869–878. [PubMed: 217353]
41. Malthouse JP, George GN, Lowe DJ, Bray RC. Biochem. J. 1981; 199:629–637. [PubMed: 6280672]
42. Dong C, Yang J, Leimkühler S, Kirk ML. lnorg. Chem. 2014; 53:7077–7079.
43. Wilson GL, Greenwood RJ, Pilbrow JR, Spence JT, Wedd AG. J. Am. Chem. Soc. 1991; 113:6803–6812.
44. Howes BD, Bray RC, Richards RL, Turner NA, Bennett B, Lowe DJ. Biochemistry. 1996; 35:1432–1443. [PubMed: 8634273]
45. Manikandan P, Choi EY, Hille R, Hoffman BM. J. Am. Chem. Soc. 2001; 123:2658–2663. [PubMed: 11456936]
46. Jones RM, Inscore FE, Hille R, Kirk ML. Inorg. Chem. 1999; 38:4963–4970. [PubMed: 11671238]
47. Shanmugam M, Zhang B, McNaughton RL, Kinney RA, Hille R, Hoffman BM. J. Am. Chem. Soc. 2010; 132:14015–14017. [PubMed: 20860357]
48. Sempombe J, Stein B, Kirk ML. Inorg. Chem. 2011; 50:10919–10928. [PubMed: 21972782]
49. Zhang B, Hemann CF, Hille R. J. Biol. Chem. 2010; 285:12571. [PubMed: 20178978]
50. Bray M R, Deeth R J. J. Chem. Soc., Dalton Trans. 1997:1267–1268.
51. Amano T, Ochi N, Sato H, Sakaki S. J. Am. Chem. Soc. 2007; 129:8131–8138. [PubMed: 17564439]
52. Mondal MS, Mitra S. Biochemistry. 1994; 33:10305–10312. [PubMed: 8068667]
53. Schopfer LM, Massey V, Nishino T. J. Biol. Chem. 1988; 263:13528–13538. [PubMed: 3166459]
54. Kim JH, Hille R. J. Biol. Chem. 1993; 268:44. [PubMed: 8380164]
55. Stockert AL, Shinde SS, Anderson RF, Hille R. J. Am. Chem. Soc. 2002; 124:14554–14555. [PubMed: 12465963]
56. Choi E-Y, Stockert AL, Leimkühler S, Hille R. J. Inorg. Biochem. 2004; 98:841–848. [PubMed: 15134930]
57. Edmondson D, Ballou D, Van Heuvelen A, Palmer G, Massey V. J. Biol. Chem. 1973; 248:6135. [PubMed: 4353632]
58. Olson JS, Ballou DP, Palmer G, Massey V. J. Biol. Chem. 1974; 249:4350–4362. [PubMed: 4367214]
59. Voityuk AA, Albert K, Romão MJ, Robert Huber a, Rösch N. Inorg. Chem. 1998; 37:176–180.
60. Ilich P, Hille R. The Journal of Physical Chemistry B. 1999; 103:5406–5412.
61. Zhang X-H, Wu Y-D. Inorg. Chem. 2005; 44:1466–1471. [PubMed: 15732988]
62. Metz S, Wang D, Thiel W. J. Am. Chem. Soc. 2009; 131:4628–4640. [PubMed: 19290633]
63. Dieterich JM, Werner H-J, Mata RA, Metz S, Thiel W. J. Chem. Phys. 2010; 132:035101. [PubMed: 20095751]
64. Bayse CA. Dalton Transactions. 2009; 2009:2306–2314. [PubMed: 19290363]
65. Metz S, Thiel W. J. Phys. Chem. B. 2010; 114:1506–1517. [PubMed: 20050623]
66. Doonan CJ, Rubie ND, Peariso K, Harris HH, Knottenbelt SZ, George GN, Young CG, Kirk ML. J. Am. Chem. Soc. 2008; 130:55–65. [PubMed: 18062689]
67. Siegbahn PEM, Shestakov AF. J. Comput. Chem. 2005; 26:888–898. [PubMed: 15834924]
68. Hofmann M, Kassube JK, Graf T. J. Biol. Inorg. Chem. 2005; 10:490–495. [PubMed: 15971074]
69. Rothery RA, Stein B, Solomonson M, Kirk ML, Weiner JH. Proc. Natl. Acad. Sci. U.S.A. 2012; 109:14773–14778. [PubMed: 22927383]

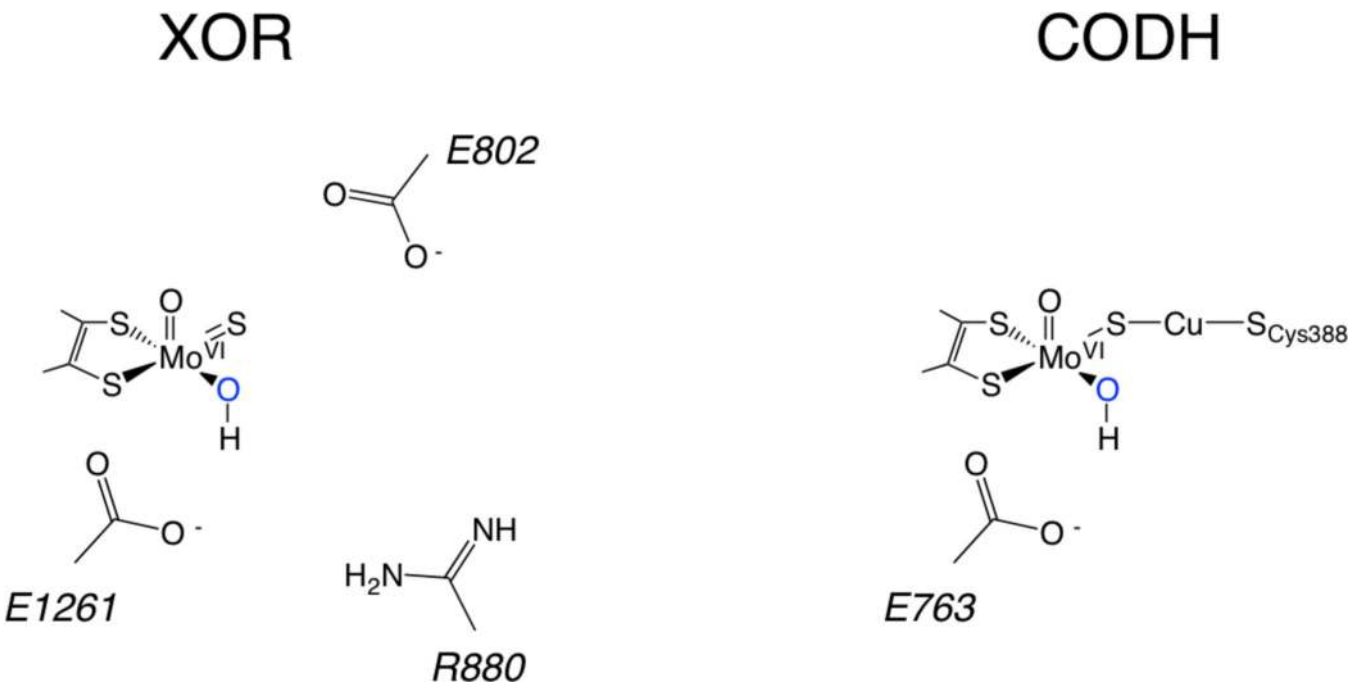


**Figure 1.**

Oxidized active site structures of XORs and CODH, including key amino acid residues. Numbering from PDB IDs 3UNC (XOR) and 1N5W (CODH). Note that the related AOs lack the equivalent of Glu802 and Arg880.

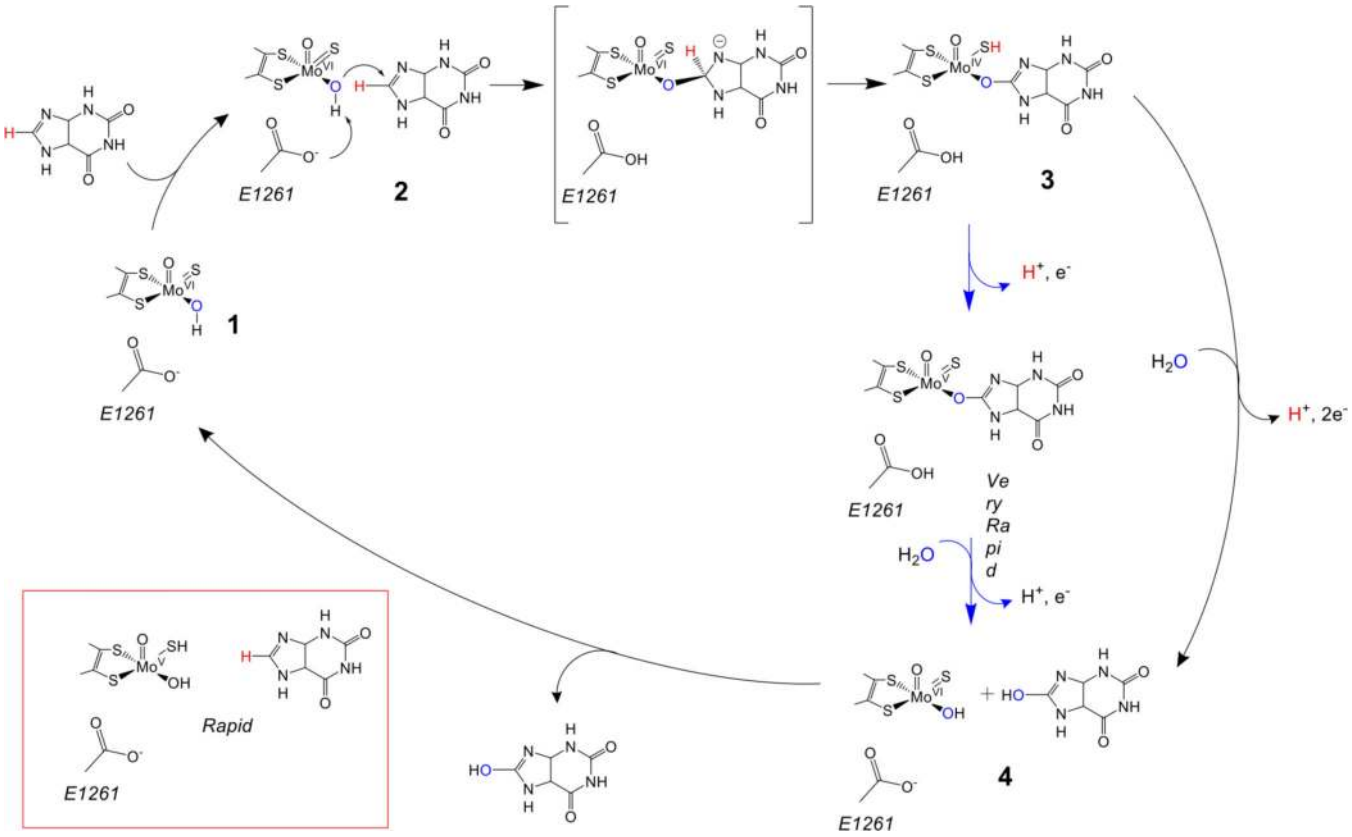


**Figure 2.**

XOR catalytic cycle for the oxidation of xanthine to uric acid. Blue arrows show the alternative reaction pathway which leads to the formation of the *very rapid* intermediate. The *rapid* form is formed by the addition of excess substrate to partially reduced enzyme.

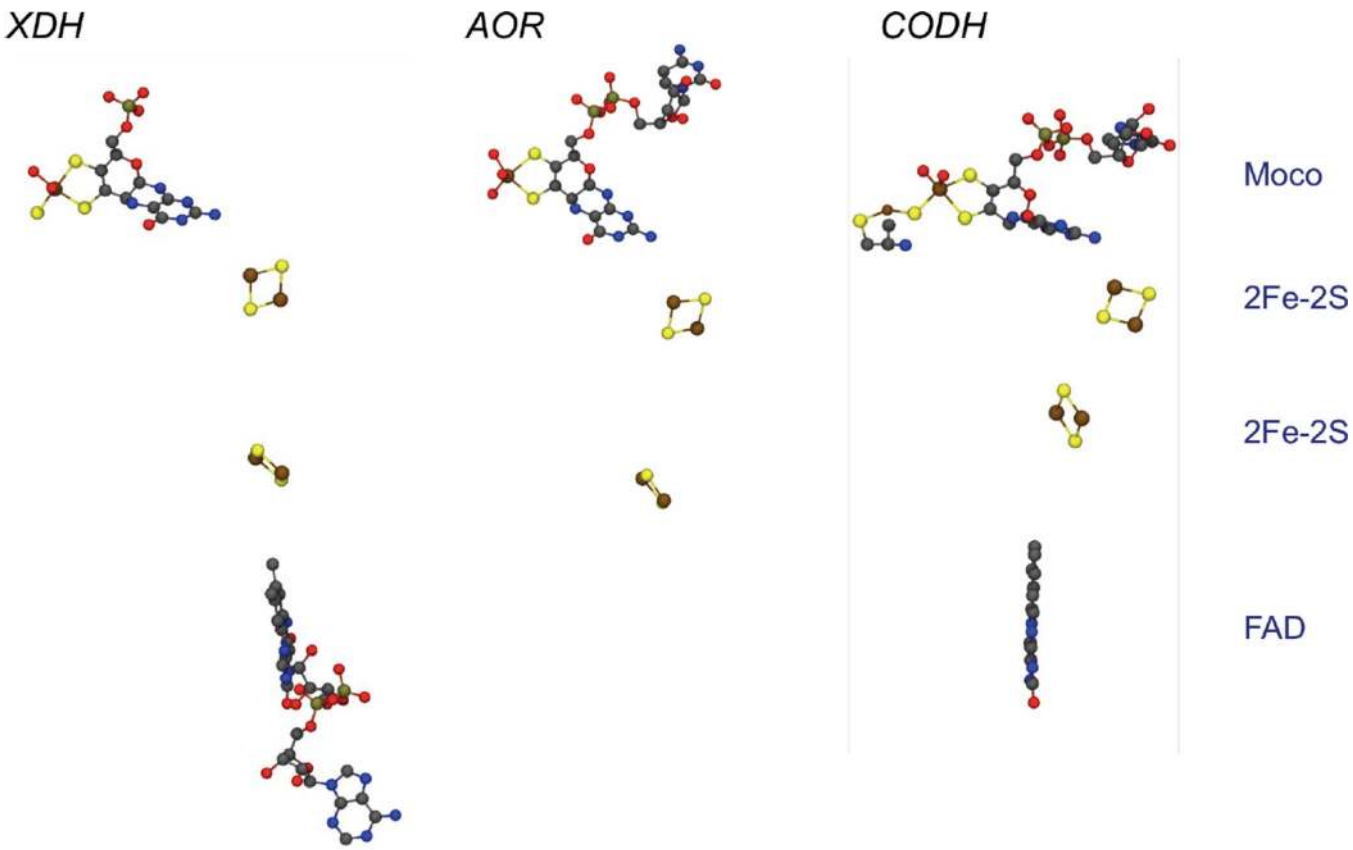


**Figure 3.**

Molybdenum hydroxylase redox cofactors: XDH (left), AO (middle), CODH (right). PBD IDs: 3UNC (XDH), 1VLB (AO), 1N5W (CODH). Note that while the aldehyde:ferredoxin oxidoreductase from *D. gigas* (shown center) lacks the FAD domain, other AOs and CODH possess FAD domains similar to the XORs.

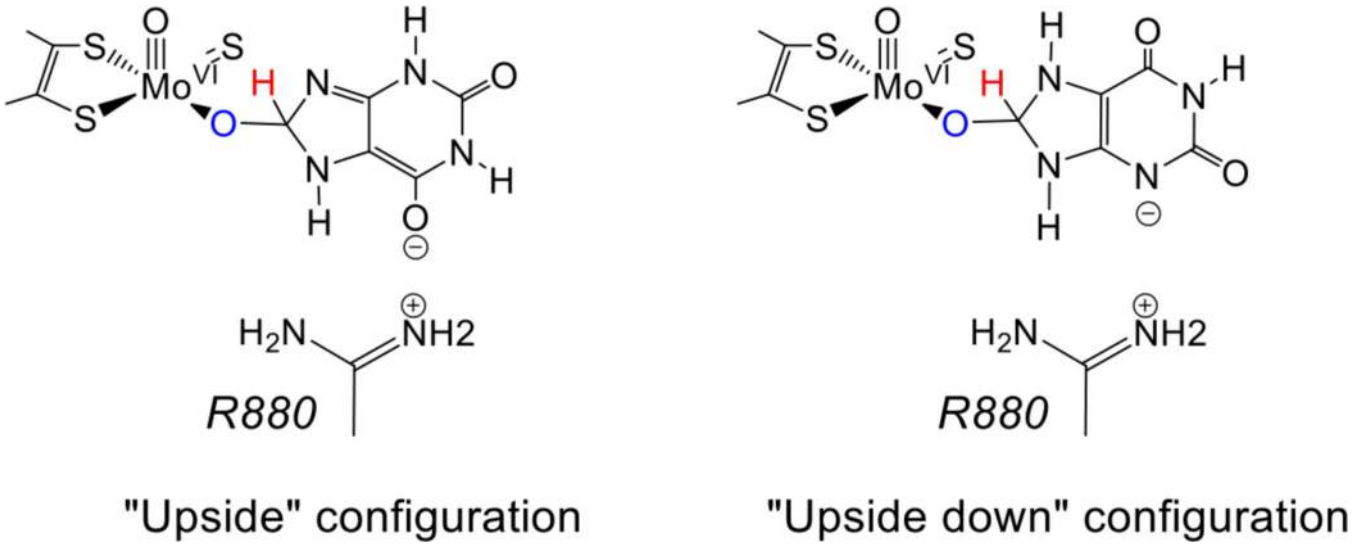


**Figure 4.**

Possible orientations of xanthine in the active site of XORs. QMMM calculations indicate that the upside configuration is more energetically favorable for catalysis[2].

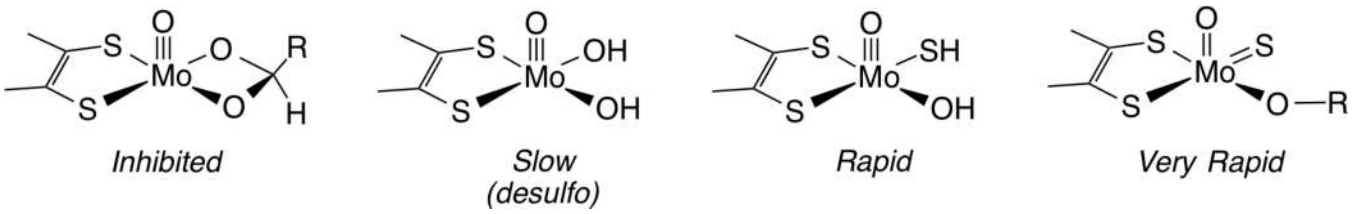


**Figure 5.**
Consensus structures for various Mo(V) XOR species studied by paramagnetic spectroscopies.

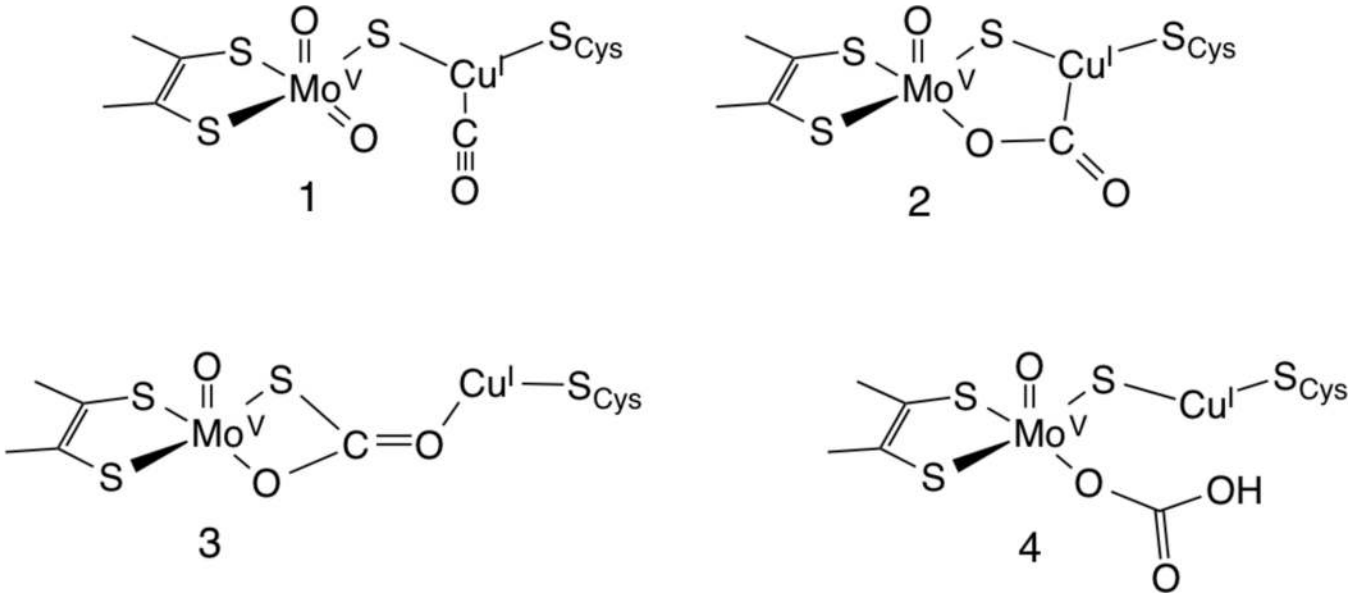


**Figure 6.**
Candidates for the EPR signal-giving species seen in reduced CODH. Adapted from reference [3].

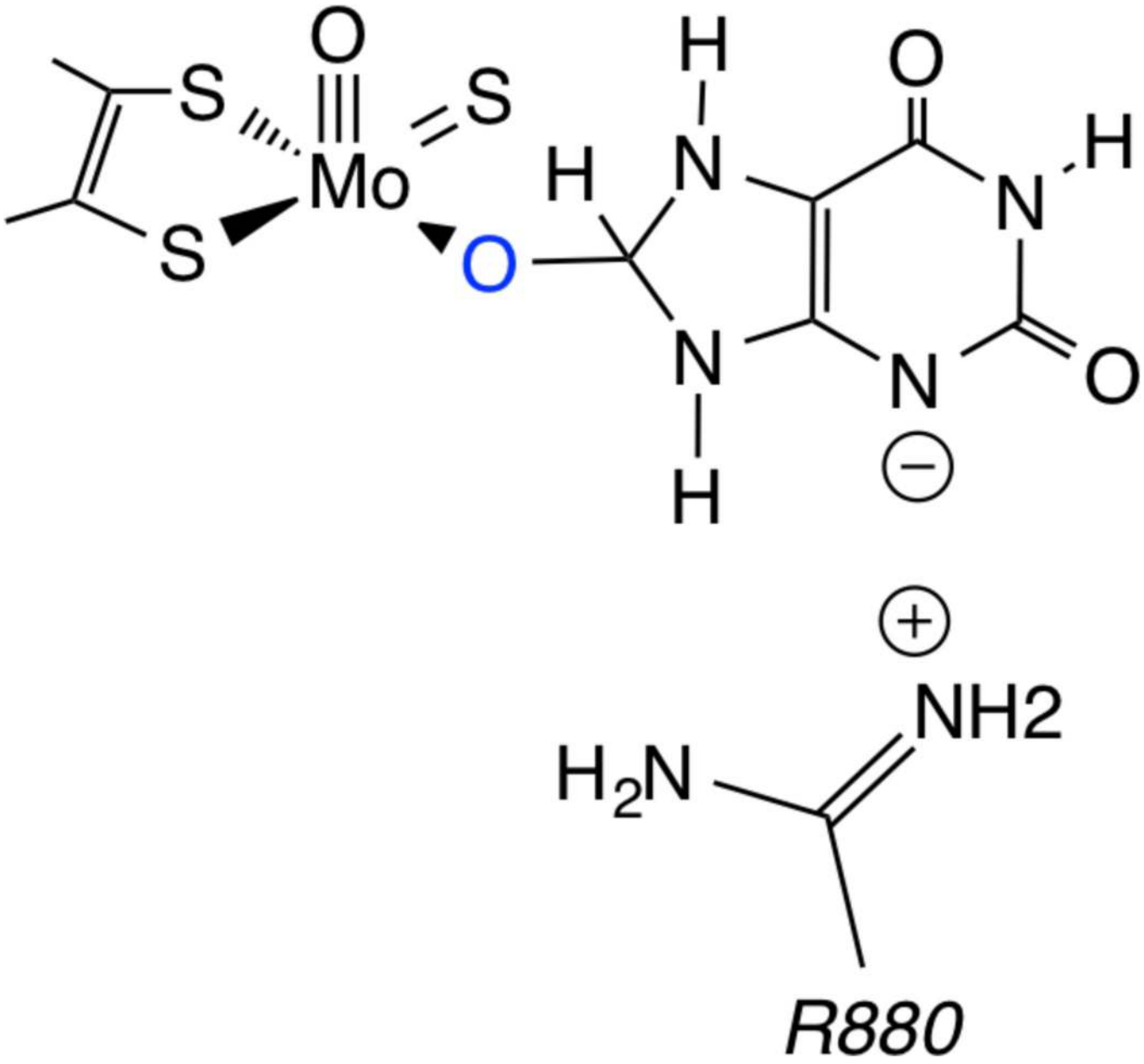


**Figure 7.**
Stabilization of excess substrate charge by Arg800, resulting in a favored “upside-down” configuration[2].

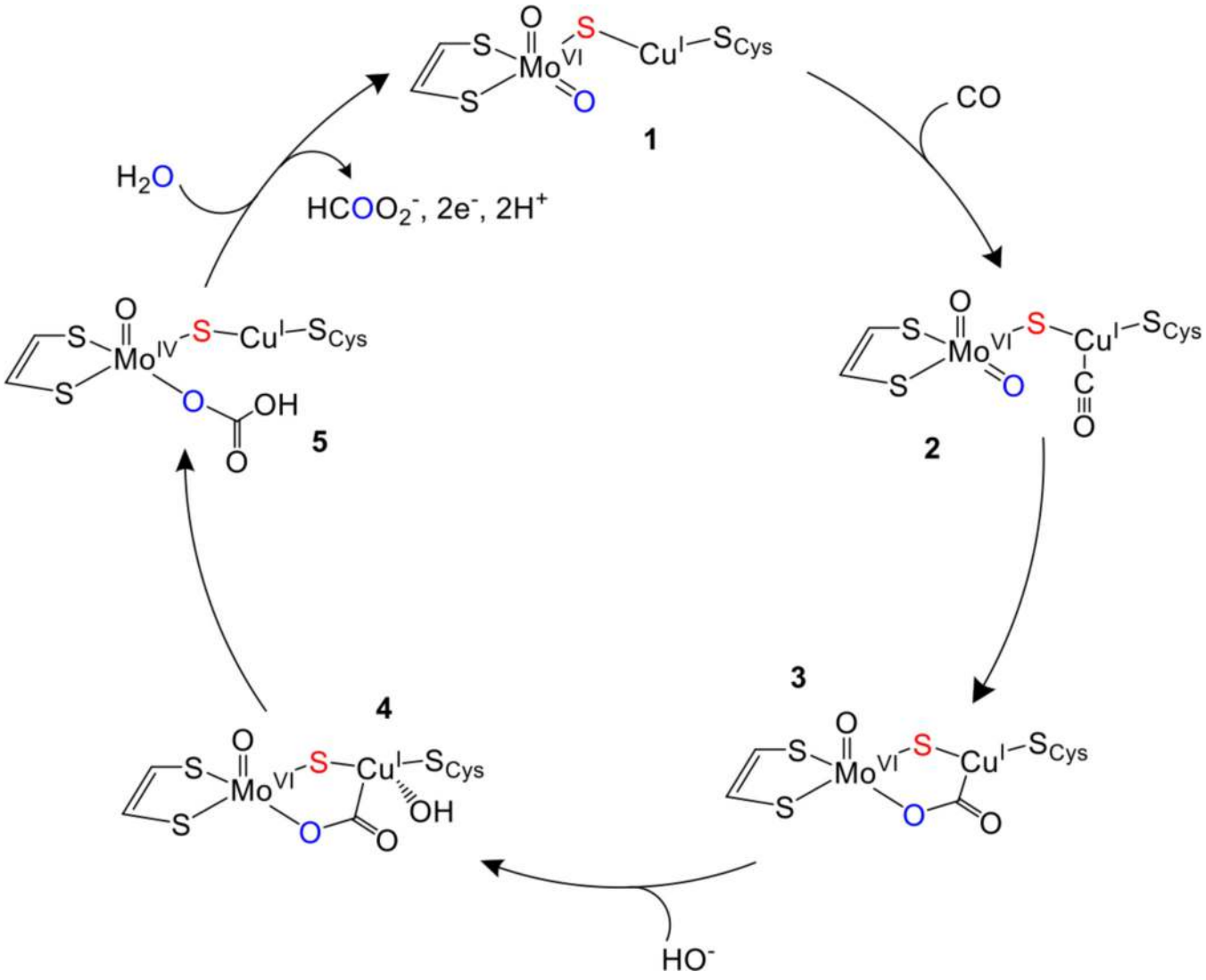


**Figure 8.**
Proposed mechanism of CODH. Adapted from ref. [1].

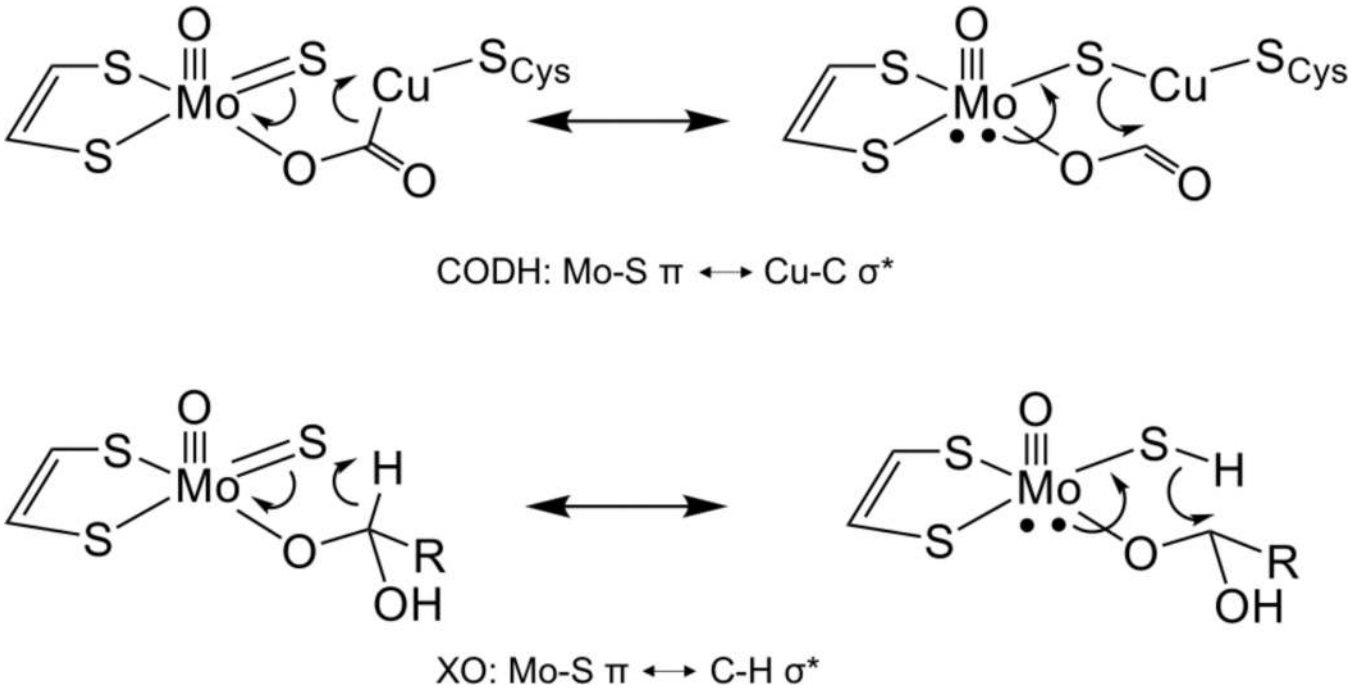


**Figure 9.**
Principle donor-acceptor contributions found in CODH and their similarity to the donor-acceptor interactions observed for XOR. Adapted from ref. [1].

## Table 1

Summary of calculated barrier heights for various XO family substrates.

| Substrate | Method | Barrier (kcal/mol) | Ref. |
|---|---|---|---|
| HCHO | B3LYP | 8.4 | [50] |
| HCHO | BP86 | 7.7 | [59] |
| $HC(=NH)NH_2$ | MP2 | 78b | [60] |
| HCHO, | B3LYP | 16.9[a] | [61] |
| | | 22.0[b] | |
| $CH_3CHO$ | | 24.5[a] | |
| | | 21.2[b] | |
| $HCONH_2$, | | 38.6[a] | |
| | | 40.0[b] | |
| $HC(=NH)NH_2$ | | 49.1[a] | |
| | | 45.4[b] | |
| $HCONH_2$ | B3LYP | 38.9[a] | [51] |
| | | 39.3[b] | |
| | CCSD(T) | 41.6[a] | |
| | | 41.1[b] | |
| $CH_3CHO$ | B3LYP/MM | 8.5 | [62] |
| $C_6H_5CHO$ | | 7.9 | |
| $CH_3CHO$ | FEP/MM | 10.8 | [63] |
| Xanthine | mPW1PW91 | 6.4 | [64] |
| Xanthine | B3LYP/MM | 13–15 | [2] |

[a]Step-wise mechanism

[b]Concerted mechanism